

## A fluorescent “Turn-ON” probe with rapid and differential response to HSA and BSA: Quantitative detection of HSA in urine

Rohini Gupta, Kamaldeep Paul\*

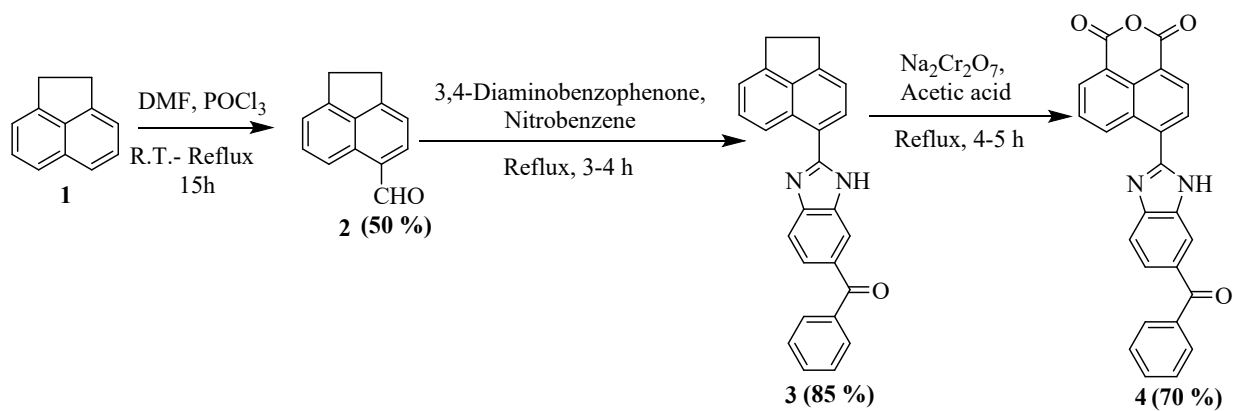
Department of Chemistry and Biochemistry, Thapar Institute of Engineering and Technology,  
Patiala-147001, India

Email: kpaul@thapar.edu

### 1. Experimental Section

#### 1.1. Synthesis of intermediate 4

To *N,N*-dimethyl formamide (2 mL, 24.8 mmol), phosphorus oxychloride (1.1 mL, 12.4 mmol) was added dropwise and stirred for 30 min under ice-bath. Then, a solution of acenaphthene (0.87 g, 5.63 mmol) in 20 ml of 1,2-dichloroethane (DCE) was added to above mixture dropwise. The reaction mixture was refluxed for 15 h, DCE from the reaction mixture was distilled off, and the reaction was cooled to room temperature and poured into ice water. The pH was adjusted to 8-9, and brown-coloured precipitates of acenaphthene-5-carbaldehyde (**2**) were filtered and dried at room temperature. After drying, column chromatography in hexane: ethyl acetate (9:1) was done to obtain 0.43 mg of pure **2** as light yellow-coloured solid with 50% yield (m.pt. 42 °C).<sup>1</sup> Acenaphthene-5-carbaldehyde **2** (500 mg, 2.74 mmol) was stirred with 3,4-diaminobenzophenone (582 mg, 2.74 mmol) in nitrobenzene at 120 °C to synthesize compound **3**. Completion of the reaction was monitored by TLC. After completion of the reaction, the mixture was cooled to room temperature and filtered after the addition of diethyl ether to obtain dark yellow-coloured precipitates in 85% yield; m.pt. 147-149 °C. Compound **3** (2 g, 5.34 mol) was further oxidized using sodium dichromate (7 g, 26.73 mol) in acetic acid for about 4-5 h to obtain compound **4**.<sup>2</sup> After completion of the reaction, the reaction mixture was poured into ice water and filtered as light-yellow precipitates was in 70% yields.



**Scheme S1:** Synthesis of intermediate **4**

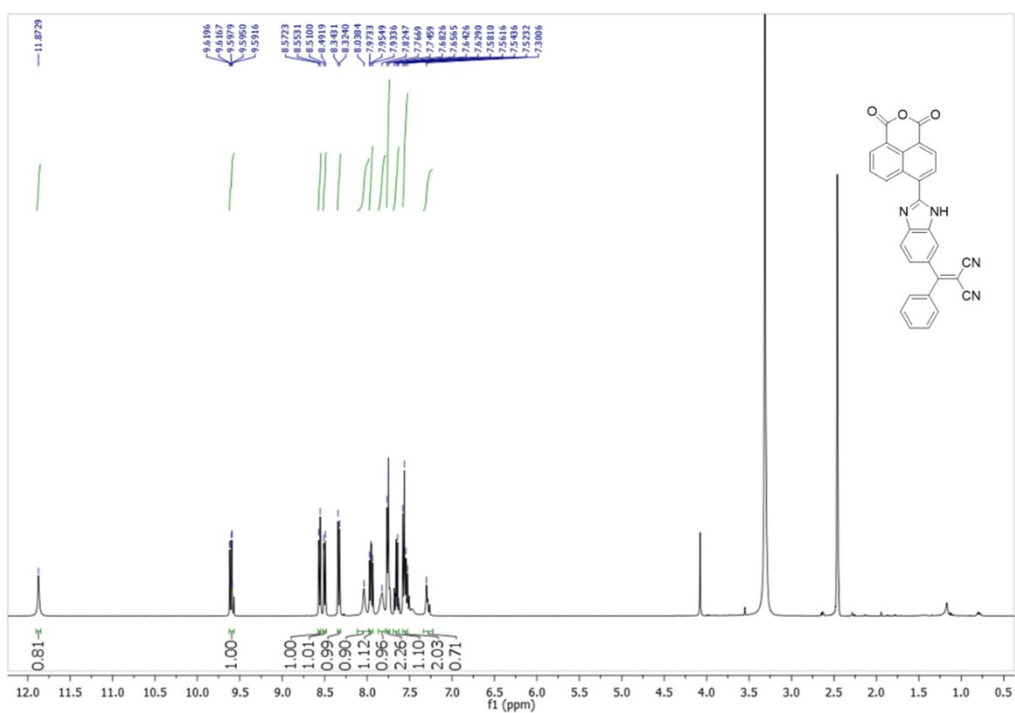


**Figure S1:**  $^1\text{H}$  NMR spectrum of 4-(6-(2,2-dicyano-1-phenylvinyl)-1*H*-benzo[*d*]imidazol-2-yl)-7-oxo-9,10-dihydro-7*H*-benzo[*de*]imidazo[2,1-*a*]isoquinoline-9,10-dicarbonitrile (**6**)

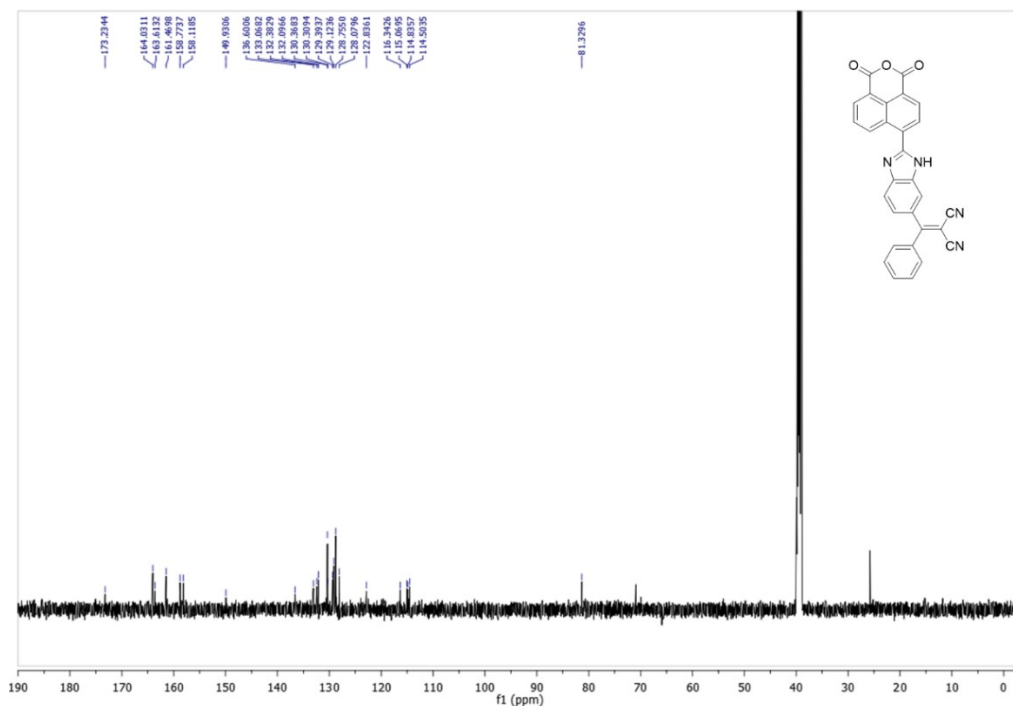


**Figure S2:** <sup>13</sup>C NMR spectrum of 4-(6-(2,2-dicyano-1-phenylvinyl)-1*H*-benzo[*d*]imidazol-2-yl)-7-oxo-9,10-dihydro-7*H*-benzo[*de*]imidazo[2,1-*a*]isoquinoline-9,10-dicarbonitrile (**6**)

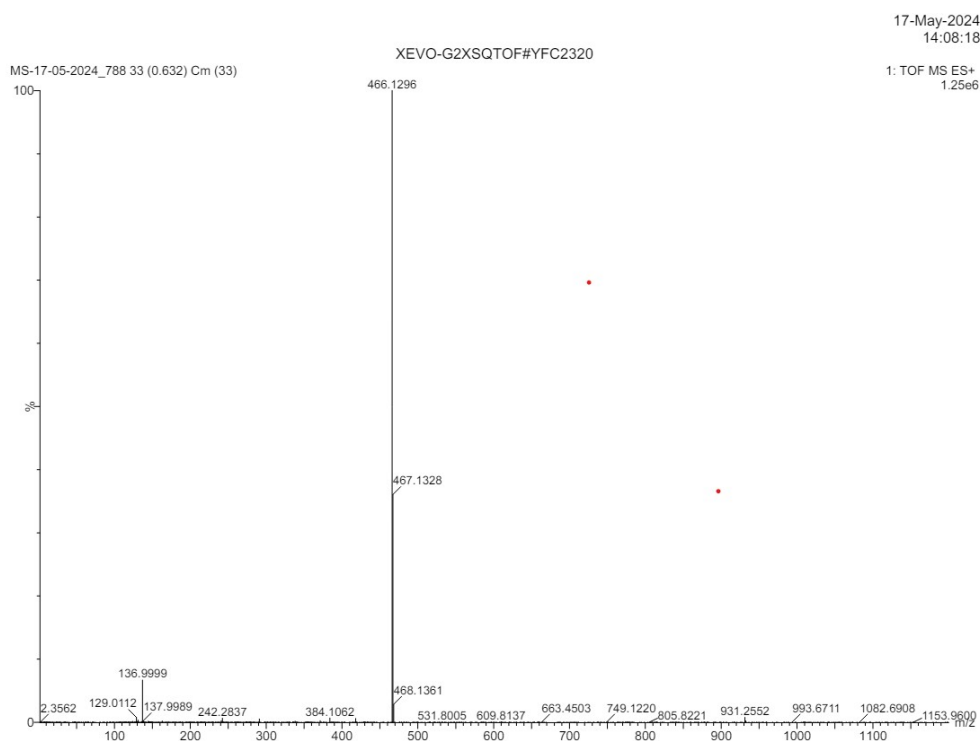


**Figure S3:** HRMS spectrum of 4-(6-(2,2-dicyano-1-phenylvinyl)-1*H*-benzo[*d*]imidazol-2-yl)-7-oxo-9,10-dihydro-7*H*-benzo[*de*]imidazo[2,1-*a*]isoquinoline-9,10-dicarbonitrile (**6**)

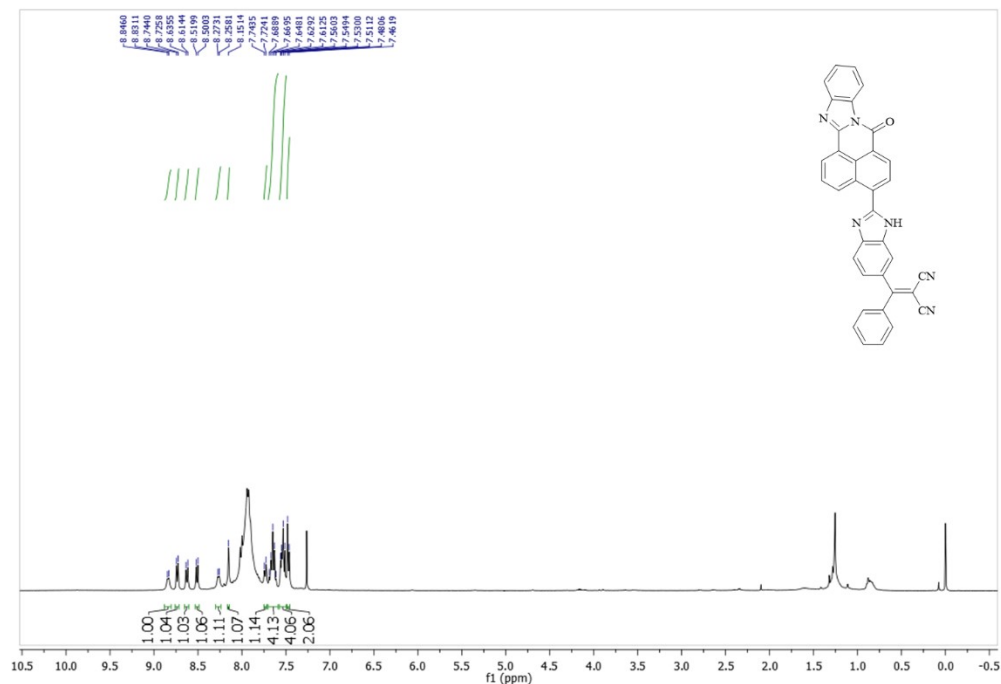


**Figure S4:**  $^1\text{H}$  NMR spectrum of 2-((2-(7-oxo-7H-benzo[de]benzo[4,5]imidazo[2,1-a]isoquinolin-4-yl)-1H-benzo[d]imidazol-6-yl)(phenyl)methylene)malononitrile (**7**)

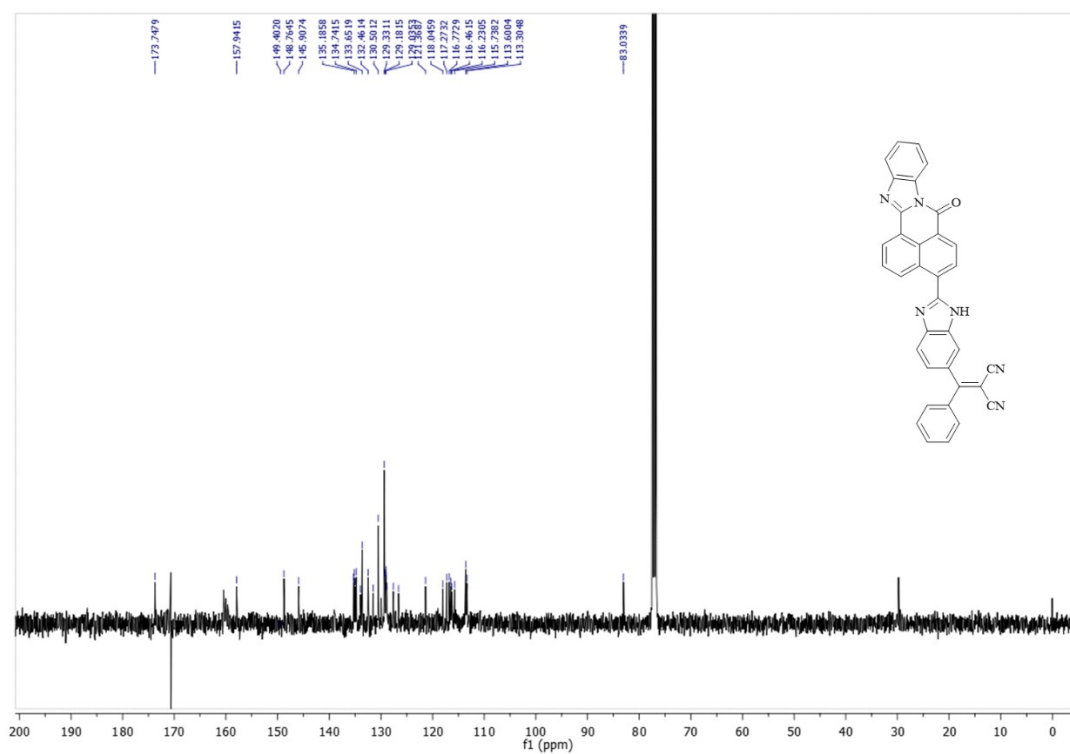


**Figure S5:**  $^{13}\text{C}$  NMR spectrum of 2-((2-(7-oxo-7H-benzo[de]benzo[4,5]imidazo[2,1-a]isoquinolin-4-yl)-1H-benzo[d]imidazol-6-yl)(phenyl)methylene)malononitrile (**7**)

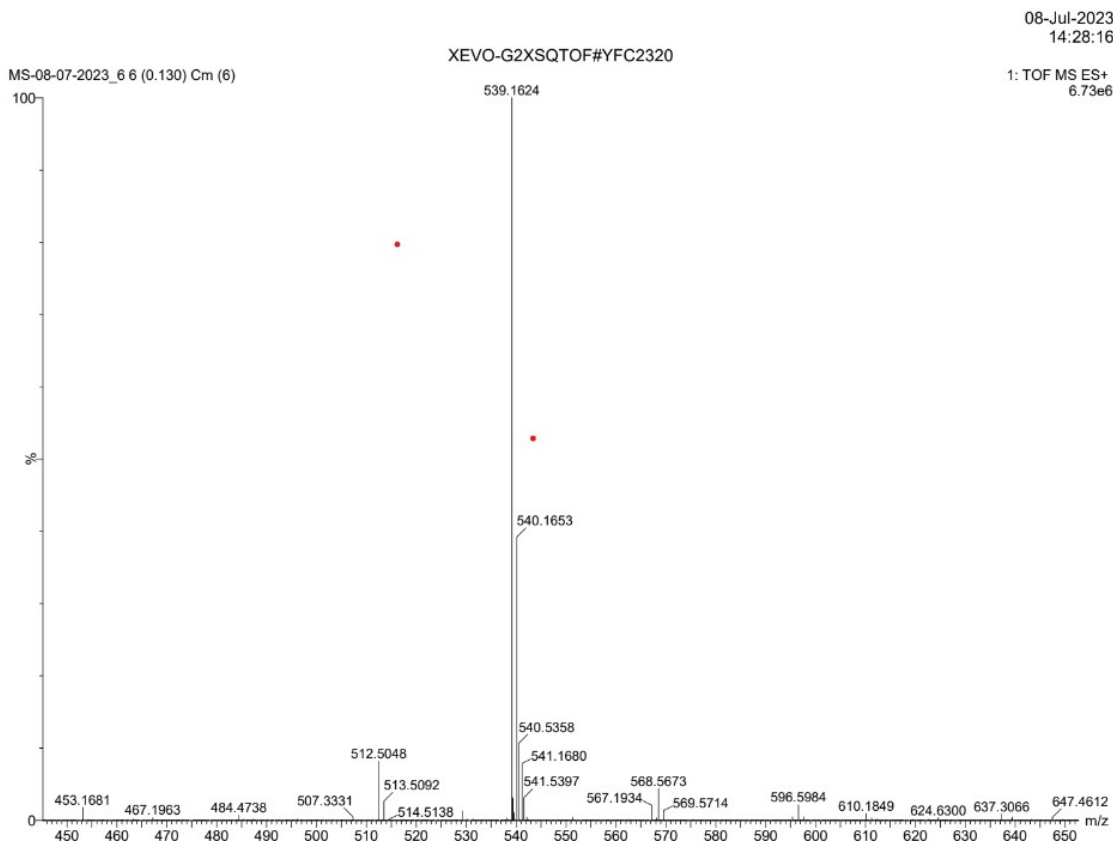


**Figure S6:** HRMS spectrum of 2-((2-(7-oxo-7*H*-benzo[*de*]benzo[4,5]imidazo[2,1-*a*]isoquinolin-4-yl)-1*H*-benzo[*d*]imidazol-6-yl)(phenyl)methylene)malononitrile (**7**)

## 1.2. Materials and preparation of solutions

Serum albumin HSA and BSA were purchased from Hi-Media and Sigma Aldrich. All other chemicals and common solvents were purchased from Spectrochem, Avra, Sigma Aldrich, and Loba Chemie and used without any further purification. The progress of the reaction was monitored using thin-layer chromatography. Purification of the compound was done by column chromatography using silica gel of mesh size 60-120. The stock solutions of probes **6** and **7** ( $10^{-3}$  M) were prepared in HPLC grade DMSO. Ultra-pure water is used throughout the experiment. All the studies were performed in a phosphate buffer (0.1M) with pH = 7.4.

## 1.3. Instruments

$^1\text{H}$  NMR and  $^{13}\text{C}$  NMR were recorded on JEOL 400 MHz instrument using  $\text{CDCl}_3$ ,  $\text{DMSO-}d_6$  and TFA as solvents. The chemical shifts are recorded in ppm in reference to TMS (tetramethyl silane). High-resolution mass spectrum were recorded using XEVO G2-XS QTOF of Waters. UV-visible absorbance measurements were performed using Shimadzu UV-2600 spectrophotometer with a

glass quartz cell of 1 cm in length at  $25 \pm 0.3$  °C. Fluorescence experiments were performed on Shimadzu RF-6000 Spectro fluorophotometer instrument using a glass quartz cuvette with 1 cm path length at  $25 \pm 0.3$  °C. The time fluorescence studies were conducted on a deltaflex™ spectrometer. To determine the particle size distribution of ligand alone and in the presence of serum albumin, dynamic light scattering experiments were performed with 90Plus Particle Size Analyzer Brookhaven at  $25 \pm 0.3$  °C.

#### **1.4. Optical measurement**

The absorbance spectra of compounds **6** (10  $\mu$ M) and **7** (10  $\mu$ M) were recorded in a 0.1 M phosphate buffer of pH 7.4 at  $25 \pm 0.3$  °C in the range of 200-800 nm. After absorbance, emission spectra of **6** and **7** were recorded in the absence and presence of serum albumin on excitation at 385 nm and 420 nm in 0.1 M phosphate buffer of pH 7.4 at  $25 \pm 0.3$  °C in the range of 400-800 nm. All the titrations were done manually by microinjector.

#### **1.5. Fluorescence quenching of HSA and BSA**

To investigate the quenching of serum albumin proteins, emission spectra of serum albumin HSA and BSA were recorded in the range of 300 to 800 nm on excitation at 280 nm in phosphate buffer solution (pH = 7.4). Fluorescence titrations were performed for both BSA and HSA on gradual addition of probe **6**. Stern Volmer equation was employed to calculate Stern-Volmer constant ( $K_{SV}$ ) and quenching constant ( $K_q$ ).

#### **1.6. Theoretical calculations**

Structure optimization and interpretation of molecular orbitals (HOMO and LUMO) were accomplished by Gaussian software using B3LYP hybrid functional and 6-311 G (d, p) basis set. Molecular docking studies were performed on AutoDock-1.5.7 to find out the forces of interaction that played major role in the differential behaviour of ligand towards HSA (1n5u) and BSA (4f5s). The final structures of probe and serum albumin complex were visualized using Discovery Studio.

#### **1.7. Time-resolved fluorescence analysis**

The lifetime decay of **6** (10  $\mu$ M) was recorded in the absence and presence of HSA and BSA (0-30  $\mu$ M) in phosphate buffer solution to analyze the complex formation and efficiency of energy transfer. The obtained lifetime decay data was fitted in bi-exponential and tri-exponential fit, and the average lifetime was calculated using the best fit model.

#### **1.8. Site marker drug displacement study**

To investigate the binding site of **6** on HSA and BSA, site marker drug displacement experiment was performed with three site marker drugs *i.e.* warfarin (site I, Subdomain IIA), ibuprofen (Site II, subdomain IIIA) and bilirubin (site III, subdomain IB). The emission spectrum of **6**∩HSA and **6**∩BSA complexes was recorded after excitation at 280 nm. Emission spectrum was recorded after the gradual addition of each of these site marker drugs in **6**-serum albumin complex solution.

### **1.9. FT-IR analysis**

*FT-IR* experiment was performed on IRTracer-100 Shimadzu to check the changes in the secondary structure of serum albumins on complexation with compound. The *FT-IR* analysis was performed to investigate the changes in the secondary structure of protein on interaction with probe **6**. *FT-IR* spectra of BSA and HSA (500 μM) in the absence and presence of **6** (250 μM) were recorded with 128 scans in 0.1 M phosphate buffer solution of pH = 7.4 at 25 ± 1 °C. All the spectra were recorded after baseline correction in the spectral region of 400-4000 cm<sup>-1</sup>. The de-convolution between 1600-1700 cm<sup>-1</sup> corresponds to the amide I peak and was performed using origin software.

### **1.10. DLS study**

Dynamic Light Scattering (DLS) experiment was performed to determine the influence of HSA and BSA on self-assembly and dis-assembly processes of **6**. The solutions of **6** (5 μM), **6** (5 μM) + HSA (50 μM), and **6** (5 μM) + BSA (50 μM) were prepared in phosphate buffer of 0.1 M at room temperature and kept undisturbed for 2 h. Then, 3 ml of each solution was taken in cuvette to record the spectra.

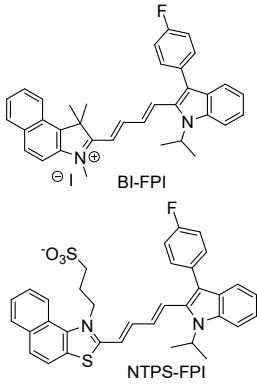
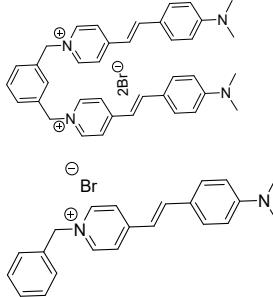
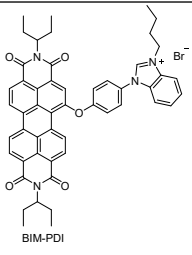
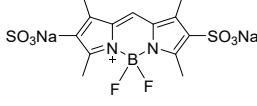
### **1.11. Procedure for MTT assay for normal cell lines**

Human embryonic kidney cells (Hek293) were cultured in DMEM along with 10% FBS, 100 mg/ml streptomycin, 100 U/ml penicillin, and 50 mM glutamine. The experiment was conducted in triplicate by seeding the cells in 96 well plates at the density of 1 × 10<sup>5</sup> in DMEM media supplemented with 10 % FBS cells. In 5 % CO<sub>2</sub> incubator cells were incubated at 37 °C. Cells were treated with five different concentrations (10, 20, 50, 80, 100 μM) of probe **6** and **7** at 37 °C for 48 h. From 5 mg/ml stock of MTT (prepared in 1\* PBS buffer) 10 μL was pipette out and added in each well then incubated at 37 °C for 4 h in the dark. The formazan crystals were dissolved in 100 μL of DMSO. Further, the amount of formazan crystal formation was measured as the difference in absorbance by Bio-Tek ELISA plate reader at 570 nm reference wavelength. All experiments were independently performed at least three times. The relative cell toxicity (%)

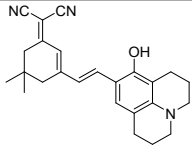
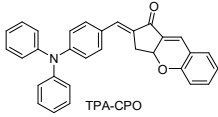
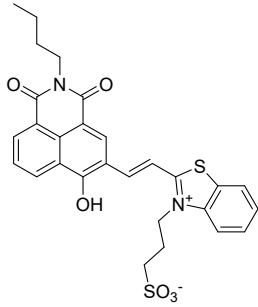
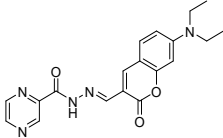
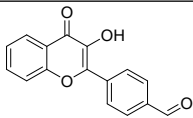
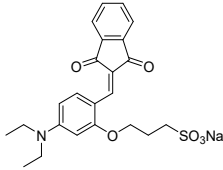
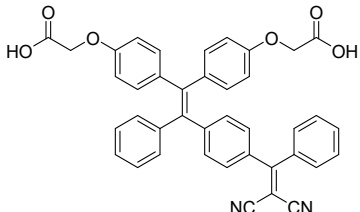
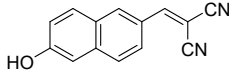
related to reference well containing only culture medium without test material was calculated using the following formula (eq. 1)

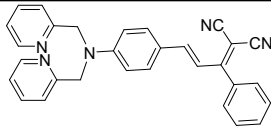
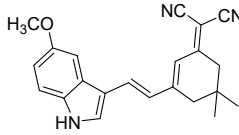
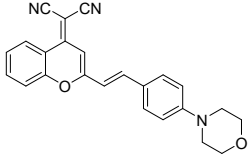
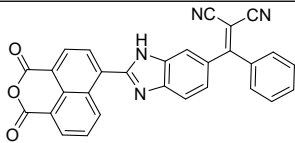
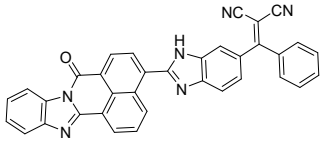
$$\% \text{ cell toxicity} = 100 - \frac{OD (\text{compound treated wells})}{OD (\text{untreated wells})} \times 100 \quad (1)$$

**Table S1:** Comparison of some important sensors for the differential detection of HSA and BSA

S.No.	Structure	Differential recognition property	Sensitive for	L.O.D.	Reference
1.	 <p>BI-FPI</p> <p>NTPS-FPI</p>	Yes	HSA	$0.01 \times 10^{-6} \text{ M}$	<i>J. Lumin.</i> <b>2018</b> , 197, 193-199
		Yes	BSA	$0.03 \times 10^{-6} \text{ M}$	
2.		Yes	HSA	$141 \times 10^{-9} \text{ M}$	<i>Mater. Chem. Front.</i> <b>2022</b> , 6, 2651-2660
		No	BSA	$14 \times 10^{-9} \text{ M}$	
			HSA	$30 \times 10^{-9} \text{ M}$	
			BSA	$90 \times 10^{-9} \text{ M}$	
3.	 <p>BIM-PDI</p>	No	HSA	$3.01 \times 10^{-6} \text{ M}$	<i>Sens. Actuators B Chem.</i> <b>2018</b> , 255, 478-489
			BSA		
4.		No	HSA	$110 \times 10^{-6} \text{ M}$	<i>J. Mol. Liq.</i> <b>2022</b> , 345, 117031-117039
			BSA	$57 \times 10^{-6} \text{ M}$	



5.		Yes	HSA	$4.64 \times 10^{-9} \text{ M}$	<i>Spectrochim. Acta A Mol. Bimol. Spectrosc.</i> <b>2022</b> , 274, 121081-121088
6.	 TPA-CPO	No	HSA	$31 \times 10^{-6} \text{ M}$	<i>Spectrochim. Acta A Mol.</i> <b>2021</b> , 205, 119409-119414
7.		Yes	HSA	$0.069 \times 10^{-6} \text{ M}$	<i>Dyes Pigm.</i> <b>2024</b> , 111893
8.		No	HSA	$1.61 \times 10^{-6} \text{ M}$	<i>J Mater Chem B.</i> <b>2020</b> , 8, 8346-8355
9.		Yes	HSA	$20.7 \times 10^{-9} \text{ M}$	<i>Spectrochim. Acta A Mol.</i> <b>2022</b> , 264, 120306-120311
10.		Yes	HSA	$1.45 \times 10^{-6} \text{ M}$	<i>Chem Asian J.</i> <b>2021</b> , 16, 1245-1252
11.		Yes	HSA	$2.7 \times 10^{-9} \text{ M}$	<i>Anal. chem.</i> , 2016, <b>88</b> , 6374-6381.
12.		Yes	HSA	$0.75 \times 10^{-9} \text{ M}$	<i>Sensor Actuat B-Chem.</i> , 2017, <b>245</b> , 923-931.

13.		Yes	HSA	$0.13 \times 10^{-6} \text{ M}$	<i>Sensor Actuat B-Chem.</i> , 2018, <b>265</b> , 204-210.
14.		Yes	HSA	$1.01 \times 10^{-9} \text{ M}$	<i>J. Mater. Chem. B.</i> , 2024, <b>12</b> , 4478-4488.
15.		Yes	HSA	$3.78 \times 10^{-3} \text{ M}$	<i>Anal. Chim. Acta.</i> , 2021, <b>1188</b> , 339201
16.	 	Yes  No	HSA BSA  —	$2.0 \times 10^{-10} \text{ M}$ $8.6 \times 10^{-10} \text{ M}$	Present Work

## 2. Supporting figures

### 2.1. Linear plots for binding constants

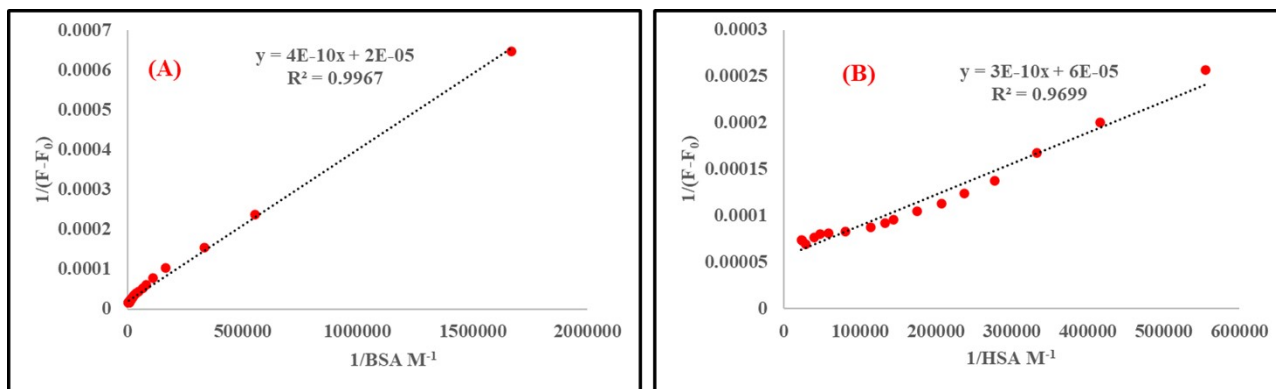


Figure S7: Benesi-Hildebrand plots for **6** on addition of (A) BSA and (B) HSA

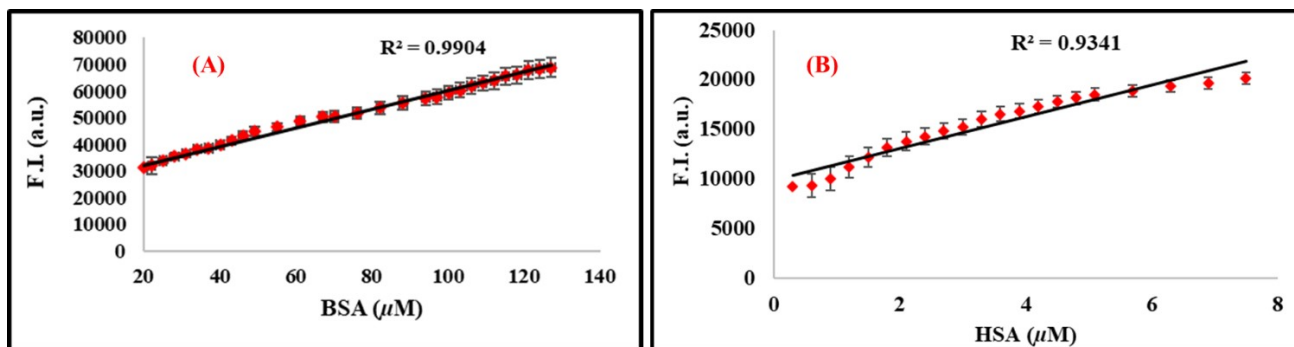


Figure S8: LOD plots of probe **6** at 475 nm for (A) BSA and (B) HSA in PBS (pH = 7.4) at 298 K

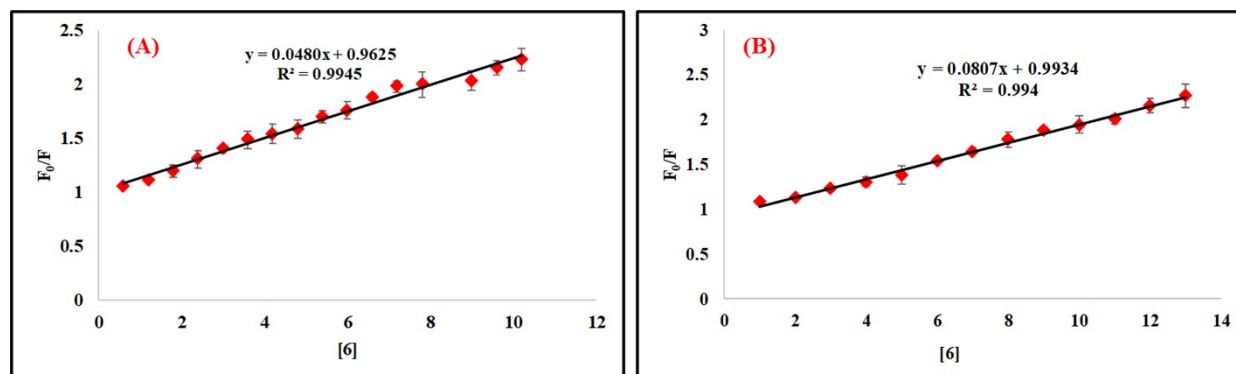
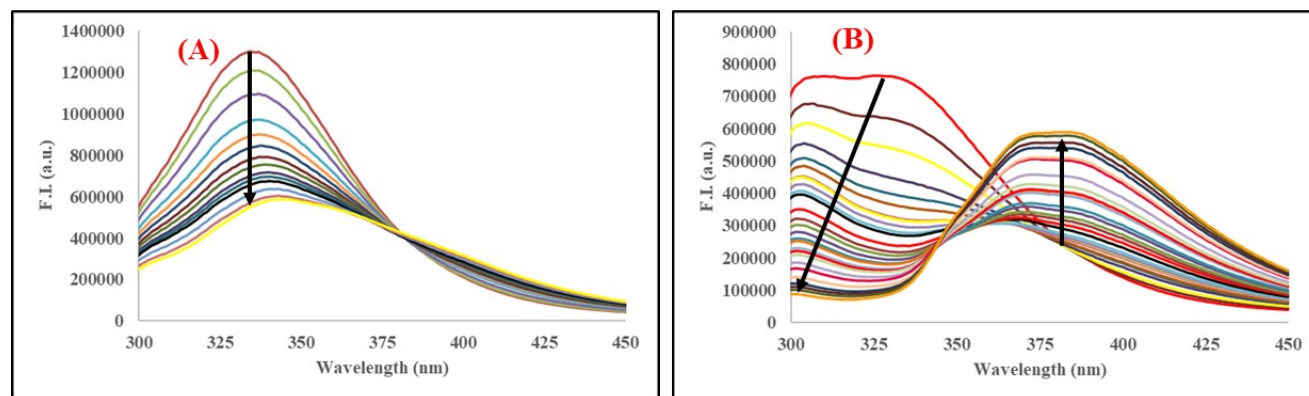


Figure S9: Stern-Volmer plots for (A) BSA and (B) HSA on addition of probe **6**

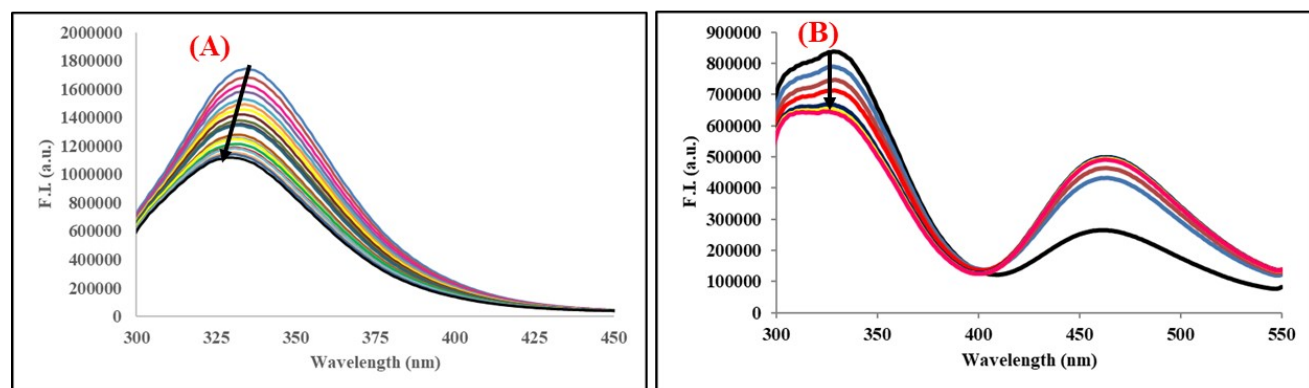
**Table S2:** Fluorescence decay profile of probe **6** and serum albumin-ligand complex systems.

System	$\tau_1$	$\alpha_1$	$\tau_2$	$\alpha_2$	$\tau_3$	$\alpha_3$	$\tau_{avg}$	$X^2$
<b>6</b>	0.58	0.24	5.52	0.33	0.11	0.41	0.24	1.07
<b>6</b> +BSA(1:1)	0.74	0.21	6.36	0.33	0.16	0.45	0.31	1.17
<b>6</b> +BSA(1:2)	1.24	0.31	7.48	0.41	0.19	0.27	0.59	0.96
<b>6</b> +BSA(1:3)	1.31	0.35	7.18	0.41	0.24	0.22	0.79	1.05
<b>6</b> +HSA(1:1)	1.13	0.23	5.77	0.33	0.18	0.42	0.50	0.94
<b>6</b> +HSA(1:2)	1.18	0.33	6.88	0.27	0.19	0.28	0.51	1.11
<b>6</b> +HSA(1:3)	1.25	0.36	7.44	0.38	0.24	0.25	0.56	1.12

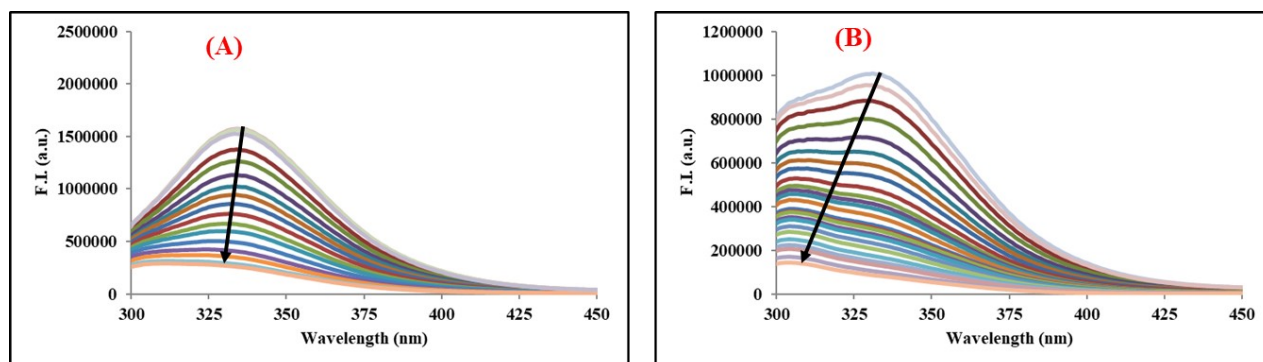
## 2.2. Site marker drug displacement studies



**Figure S10:** Change in emission spectra of (A) BSA (10  $\mu\text{M}$ ) and (B) HSA (10  $\mu\text{M}$ ) and probe complex (10  $\mu\text{M}$ ) on addition of warfarin

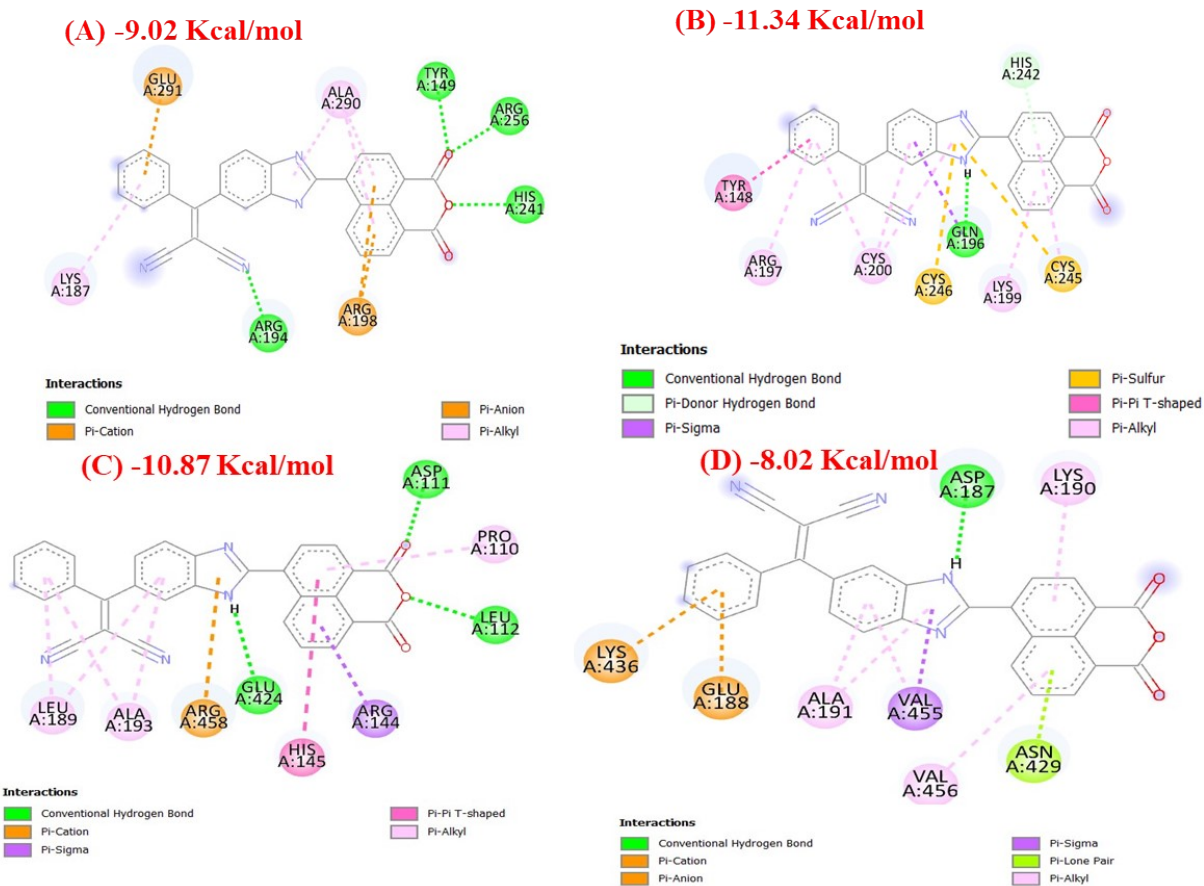


**Figure S11:** Change in emission spectra of (A) BSA (10  $\mu$ M) and (B) HSA (10  $\mu$ M) and probe complex (10  $\mu$ M) on addition of ibuprofen



**Figure S12:** Change in emission spectra of (A) BSA (10  $\mu$ M) and (B) HSA (10  $\mu$ M) and ligand complex (10  $\mu$ M) on addition of bilirubin

### 2.3. Molecular docking studies



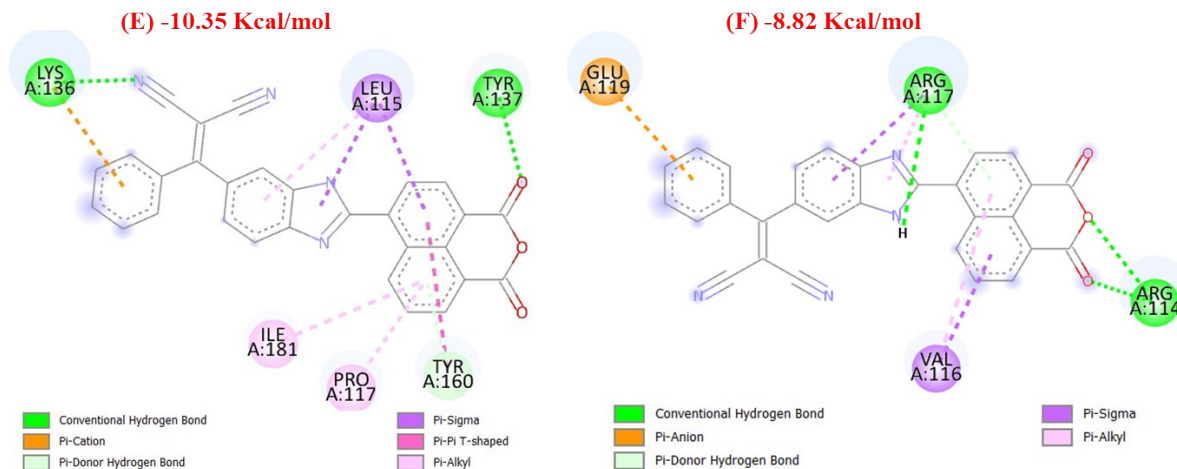


**Figure S13:** 2-D view of amino acid residues surrounding **6**: suldow site 1 (warfarin site), suldow site 2 (Ibuprofen) and suldow site 3 (bilirubin binding site), (A), (C), (E) for HSA (pdb: 1n5u) and (B), (D) and (F) for BSA (pdb: 4f5s).

**Table S3:** Amino acid residue involved in the ligand-protein interaction and free binding energy

Serial	$\Delta G$ (kcal mol <sup>-1</sup> )	PDB ID	Site	Amino acid residue involved in interaction	Type of interaction	Bond distance
1	-7.87	4f5s	Subdomain IIA	Glu291 Lys187 Arg194 Arg198 Arg290 Tyr149 Arg256 His241	$\pi$ -Cation $\pi$ -Alkyl H-Bond $\pi$ -Anion $\pi$ -Alkyl H-Bond H-Bond H-Bond	3.27 5.46 1.98 3.59, 4.41 5.26, 3.17, 4.11 1.99 2.36 2.21
2	-10.87	4f5s	Subdomain IIIA	Asp111 Pro110 Leu112	H-Bond $\pi$ -Alkyl H-Bond	1.88 5.23 2.23

				Arg144 His145 Glu424 Arg458 Ala193 Leu189	$\pi$ -Sigma $\pi$ - $\pi$ T- shaped H-Bond $\pi$ -Cation $\pi$ -Alkyl $\pi$ -Alkyl	3.98 5.90 2.28 3.58 4.76, 5.49 4.46, 4.89
3	-10.35	4f5s	Subdomain IB	Lys136 Leu115 Tyr137 Tyr160 Pro117 Ile181	H-Bond, $\pi$ -Cation $\pi$ -Sigma $\pi$ -Alkyl H-Bond H-Bond $\pi$ -Alkyl $\pi$ -alkyl	2.6, 4.17 3.95, 3.47, 3.90 4.71 2.18 2.59 4.51 4.48
4	-11.34	1n5u	Subdomain IIA	His242 Cys245 Lys199 Gln196 Cys246 Cys200 Arg197 Tyr148	Donor H- Bond $\pi$ -Sulfur $\pi$ -Alkyl H-Bond, $\pi$ -Sigma $\pi$ -Sulfur $\pi$ -Alkyl $\pi$ -Alkyl $\pi$ - $\pi$ T- shaped	2.42 5.17 4.19 2.24, 3.99 4.47 4.48, 4.61, 5.09 4.95 4.84
5	-8.02	1n5u	Subdomain IIIA	Asp187 Lys190 Asn429 Val456 Val455	H-Bond $\pi$ -Alkyl $\pi$ -Lone pair $\pi$ -Alkyl $\pi$ -Alkyl, $\pi$ -	2.61 2.71 4.62 4.58, 3.56

				Ala191 Glu188 Lys436	Sigma $\pi$ -Alkyl $\pi$ -Sulfur $\pi$ -Sulfur	4.35, 4.48 4.87 4.05
6	-8.82	1n5u	Subdomain IB	Arg117  Arg114 Val116 Glu119	$\pi$ -Sigma, $\pi$ -alkyl, H-Bond, $\pi$ -Donor, H-Bond H-Bond $\pi$ -Alkyl, $\pi$ - Sigma $\pi$ -Anion	3.38, 3.50, 4.04 2.49 2.81 2.12, 2.16 4.94, 3.76 3.70

#### References:

1. Y. Feng, L. Bai, S. Wang, X. Kong, L. Cong, Q. Zhao, Q. Yang, and Y. L., *Chem. Res. Chin. Univ.*, 2017, **33**, 534-539.